Prospects of Gallium Nitride Based DD-IMPATT Devices as Potential High-Power THz Source

P. R. TRIPATHY

Department of Electronics and Communication Engineering
Gandhi Engineering College Bhubaneswar

Abstract- In this paper the prospects of impact avalanche transit time (IMPATT) devices based on wide band gap semiconductor material gallium nitride (GaN) has been explored for operation at terahertz frequencies. Drift-Diffusion model is used to design double drift (DD) IMPATT by taking wurtzite type GaN at 1.0 THz and 1.5 THz frequencies. The performance modulation of Wz-GaN based diode is simulated by using advanced computer simulation methods by taking the experimental materials parameters and optimized at different current density and doping profile. It is observed from the results that RF power density of 502.14 mW with efficiency of 13.5% at 1.00 THz and 194.23 mW with 12.4 % at 1.5 THz frequency. The simulation results and the proposed experimental methodology can be utilized Wz-GaN based IMPATT oscillator for terahertz communication.

I. Introduction

Recently, Terahertz (THz) frequency domain i.e., between 1 millimeter (300 GHz) and 100 micrometers (3 THz) inherent advantages and potential for military & security as well as industry relevant applications as an important driver of interest in this science and technology area [1-3]. Since the last decade, scientists working in this area have been showing interest in developing solid-state sources that may be employed as a high-power terahertz source. Among all the solid-state sources, impact avalanche transit time (IMPATT) diodes have already emerged as the most powerful solid-state source, and are now widely used in various civilian and space communication systems, as well as in high-power radars, missile seekers, etc [4-7]. However, the terahertz region is unapproachable by conventional Si and GaAs based IMPATT devices, because the material parameters of these semiconductors impose restrictions on terahertz-frequency operation. Wide-band gap (WBG) semiconductors such as III–V gallium nitride (GaN) offer interesting alternatives to traditional Si and GaAs due to the possibility of operation with a higher output power (P_{RF}) resulting from increased critical field (E_C), higher band-gap energy (E_g), higher saturation velocity, and much better thermal conductivity (Table 1) [12]. A higher value of E_c results in devices with higher breakdown voltage (V_B), which enhances the output-power level of the devices. With a high value of E_C, a much higher doping level can be achieved. Another consequence of a higher electric field and a higher doping density is the width reduction in the drift region. Thus, not only the high-power but also the high-frequency (terahertz) operation capability is expected from Wz-GaN based IMPATT devices. One of the important advantages of GaN over SiC is the ability to form heterojunctions. The fact that GaN together with InN and AlN, allows the formation of heterostructures provides some interesting device possibilities. The III-Nitride family consists of the binary semiconductors; InN, AlN and GaN, and the ternaries composed of them, $Al_xG_{1-x}N$ and $In_x\ Al_{1-x}N$. GaN can be grown in two phases: zinc-blende (cubic) and wurtzite (hexagonal), while the remaining III-Nitride semiconductors only have the wurtzite polytype. The III-Nitride family of materials has gain interest in both opto-electronic and high-power solid-state devices. Their technological immaturity is mainly due to fabrication problems; however in recent years, advances have been made in the wurtzite-phase versions. Commercial GaN based devices

are grown heteroepitaxially on substrates like Sapphire and SiC [8-11]. Recently, Si has been considered as a substrate for GaN growth for its low price, high crystalline quality and potential capabilities for integration with traditional Si-based electronic technology. MOCVD has become the technique of choice for the epitaxial growth of GaN material and devices [Pearton (2000)]. In MOCVD growth, Si and Mg are used as donor and acceptor impurities, respectively. This broad spectrum of applications has led some to predict that GaN will eventually become the third most important semiconductor material, behind Si and GaAs. A. K. Panda et al. (2001) designed and studied the performances of GaN based IMPATTs in the D-band. The maximum power that may be obtained from their designed diode was 3.775 W with an efficiency of 12.5%. Moreover, their study predicted that the wurtzite-phase GaN based IMPATT is better than its zinc-blend counterpart, as far as breakdown voltage, power output and efficiency are concerned. Later, Reklaitis et al. (2005) performed a Monte Carlo simulation of Wz-GaN based near-terahertz IMPATT diode. Their analysis predicted that the device may generate a RF power of ~ 3W at 0.45 THz with an efficiency of 18%. Thus the author has studied the DC and Terahertz -frequency characteristics of the GaN based flat types IMPATT devices at elevated junction temperature.

2. COMPUTER SIMULATION TECHNIQUE

Double-drift IMPATT devices are designed and optimized by using a generalized double iterative simulation technique developed by the author [11]. For the present analysis, a flat profile DDR ($n^{++}npp^{++}$) structure is considered, where n^{++} and p^{++} are highly doped substrate shown in figure 1. The material and physical parameters have been taken from recent experimental data [12]. In the DC method, the computation starts from the field maximum near the metallurgical junction. The distribution of dc electric field and carrier currents in the depletion layer, which involves iteration over the magnitude of electric field maximum (E_m) and its location in the depletion layer of the diode by simultaneous solution of Poission and carrier continuity equations at each point in the depletion layer. The field boundary conditions are given by

$$E(-x_1)= 0 \qquad E(+x_2)= 0 \qquad (1)$$

Here $-x_1$ and x_2 represents the edges of the depletion layer in n and p regions respectively. The DC analysis also gives the carrier concentration profile or the carrier current density profile which indicates the avalanche zone width within which a maximum of 95% carrier multiplication takes place and the width of drift zone where there is marginal carrier multiplication. The electric field can be integrated over the entire avalanche zone to compute the avalanche voltage drop (V_A) and drift zone to compute the drift voltage drop (V_D). Then the total breakdown voltage V_B of the diode is calculated from the expression $V_B = V_A+V_D$. The conversion efficiency from DC to RF is computed following Scharfetter and Gummel [13] as,

$$\eta = \frac{V_D}{\pi V_B} \qquad (2)$$

Though this expression is an approximate one, this can be taken as an indicative parameter of device performance. The DC analysis includes several realistic parameters under various structural and operating conditions along with diffusion current and tunneling current which have been carried out by us to be presented later. Later, the small signal analysis was extended by Gilden and Hines [14], by considering the entire depletion zone to be consisting of avalanche zone, drift zone and an inactive zone in which the avalanche zone is assumed to be thin across the junction having high electric field where as the drift zone with low field near the edges of the junction by assuming the equal ionization rate coefficients and saturated drift velocities of charge carriers.

A small-signal ac field $\tilde{e}$ is superimposed on the DC field [14] for the small signal analysis of the IMPATT diode such that the ac avalanche current density $\tilde{J}_a$ is given by,

$$\tilde{J}_a = \frac{2\alpha' x_A J_0 \tilde{e}}{i\omega\tau_a} \quad (3)$$

where ω is the angular frequency of $\tilde{e}$, x_A is the width of avalanche region, time $\tau_a = x_A/v_s$, α' is the field derivative of ionization rate, J_o is the total current density.

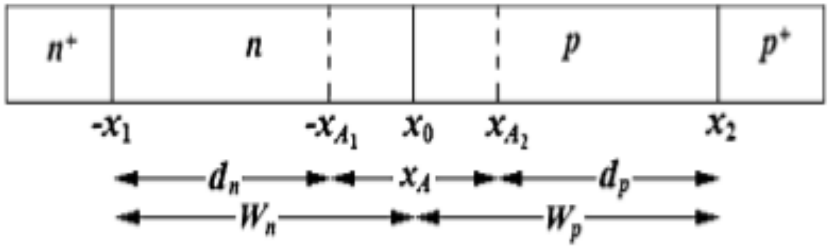

Figure 1. One-dimensional model of DDR IMPATT Devices

And the total diode impedance Z is given by,

$$Z = R_S + \frac{l_d}{\omega\varepsilon}\left\{1-\frac{\omega^2}{\omega_a^2}\right\}^{-1}\left\{\frac{1-\cos\theta}{\theta}\right\} + \frac{1}{i\omega\varepsilon}\left[x_A\left\{1-\frac{\omega_a^2}{\omega^2}\right\}^{-1} + l_d\left\{1-\left(1-\frac{\omega^2}{\omega_a^2}\right)^{-1}\right\}\frac{\sin\theta}{\theta}\right]$$

(4)

where $\omega_a = 2\alpha' x_A J_o/\varepsilon\tau_a$ is the avalanche frequency, $\theta = (\omega l_d)/v_s$, l_d is the length of the drift region, ε is the permittivity of semiconductor, R_S is the parasitic series positive resistance of the diode. The real part of the equation (4) suggests the negative value of the diode impedance for frequency greater than the avalanche frequency ($\omega > \omega_a$) where as it is positive for frequencies less than ($\omega < \omega_a$) avalanche frequency. The small signal parameters like diode negative conductance, diode negative resistance, the optimum frequency, the Q-factor, Bandwidth etc. can be computed from this analysis. Finally the RF Power output can be calculated by using the relation

$$P_{RF} = (V_B/2)^2 x G_P A/2 \quad (5)$$

where G_p is the peak conductance at peak frequency and A is the area of the diode [9].

3. RESULTS AND DISCUSSIONS

The optimized design parameters with current density of the double drift IMPATT diode is shown in table 2. Table 3 shows the dc and small signal results at different terahertz frequencies. It has been observed from the table 2 that when the designed frequency is more the current density also increases. Table shows that when the frequency increases, peak electric field (E) increases with breakdown voltage (V_B), avalanche voltage (V_A), efficiency (η) decreases. But the width (X_A/W), negative conductance (G_P), susceptance (B_P) increases when the operating frequency increases from 1.0 THz to 1.5 THz. The maximum breakdown voltage of 41.9 V is obtained at a current density of $1.1x10^9$ A/m^2 at 1.0 THz, where as 31.5V is obtained at a current density of $1.6x10^9$ A/m^2 at 1.5 THz frequency. The RF power output increases at 1.0 THz frequency of about 502.14 mW as compared to other frequencies. The mean square noise voltage is also calculated for different frequency of operation. It is seen that noise voltage and Noise Measure obtained from this Wz-GaN based IMPATT and is significantly high at 1.0 THz as compared to 1.5 THz frequency.

Table 1. Material and Physical parameters of semiconductor materials at 300 K [12]

Property	**Si**	**GaAs**	**Wz-GaN**
Band gap, E_g(eV)	1.12	1.43	3.39
Dielectric constant, ε_r *a*	11.9	13.1	9.0

Electric breakdown field, E_c(V/m)	3.0	4.0	30
Electron mobility, μ_n (m^2/V·s)	1500	850	1600
Hole mobility, μ_p(m^2/V·s)	600	400	280
Thermal conductivity, λ (W/cm·K)	150	46	225.0
Saturated drift velocity, v_{sat}(×10^7 cm/s)	1.0	1.2	2.5

Table 2. Design parameters of Wz-GaN based IMPATT diode at different THz frequencies

Frequency (THz)	**W_n (nm)**	**W_p (nm)**	**N_D (×10^{23}/m^3)**	**N_A (×10^{23}/m^3)**	**Current Density (x10^9A/m^2)**
1.0	185.0	185.0	7.1	7.2	1.1
1.5	130.0	130.0	10.0	10.5	1.6

Table 3. DC and small-signal properties of Wz-GaN based IMPATT diode at different THz frequencies

Frequency (THz)	**E(×10^8 V/m)**	**V_B(V)**	**V_A(V)**	**η (%)**	**X_A/W (%)**	**$-G_P$ (×10^8 S/m^2)**	**$-B_P$ (×10^8 S/m^2)**	**Q_P =-(B_P/G_P)**	**$-Z_R$ (×10^{-9}Ω/m^2)**	**P_{RF} (mW)**
1.0	21.5	41.9	24.4	13.5	40.6	47.16	181.2	3.84	0.141	502.14
1.5	22.5	31.5	19.8	12.4	46.1	126.9	409.4	3.22	0.067	194.23

4. CONCLUSION

A detailed comparative analysis of the wide band gap Wz-GaN based IMPATT devices in the terahertz regime has been reported. This paper reveals that as a high power terahertz source, Wz-GaN IMPATT device is more potential candidate than other materials. The simulation results and experimental feasibility provide useful information for application in interstellar explorers.

References

[1] P. H. Siegel, Terahertz technology in biology and medicine, IEEE Trans Microwave Theory Tech., Vol. 52 (2004), pp. 2438–2447.

[2] José Millán et al, Wide Band Gap Semiconductor Devices for Power Electronics, AUTOMATIKA, Vol. 53(2) (2012), pp.107–116.

[3] B. Ferguson and X.C Zchang , Material for Terahertz Science and Technology , Nature Matter, Vol.1 (2002), pp-26-33.

[4] Sitesh Kumar Roy and Monojit Mitra, Microwave Semiconductor Devices, PHI Learning Private Limited, Forth edition, (2008)

[5] V. V. Buniatyan and V. M. Aroutiounian, "Wide gap semiconductor microwave devices", Journal of Physics D, Apply. Phys., Vol. 40 (20) (2007), pp. 6355-6385.

[6] K. S. Boutros, S. Chandrasekaran, W. B. Luo, V. Mehrotra, GaN Switching Devices for High- Frequency, KW Power Conversion, Proc. International Symp. Power Devices and ICs (ISPSD-2006), Italy, (2006), pp. 321-323.

[7] A. Agarwal, Advanced in SiC MOSFET Performance, ECPE SiC & GaN Forum: Potential of Wide Band gap Semiconductors in Power Electronics Applications, Birmingham, UK, (2011)

[8] S. J. Peatron, J. C. Zolper, R. J. Shul and F. Ren, "GaN: Processing, defects, and devices", Journal of Applied Physics, Vol. 86 (1999), pp. 1-78.

[9] I. H. Oguzman, E. Belloti, K.F. Brennan, J. Kolnik, R.Wang, P.P.Buden Theory of hole initiated impact ionization in bulk Zinc blende and wurtzite GaN, J. Appl. Phys., Vol. 81 (2) (1997), pp. 7827-7836.

[10] J. D. Albrecht et al., Electronic transport characteristics of GaN for high temperature device modeling, J. Appl. Phys., Vol. 83 (1998), pp. 4777-4781.

[11] P. R. Tripathy et al, THz Performance of Nano Dimension Si, GaAs and InP ATT Devices, Journal of Computational and Theoretical Nanoscience, Vol. 20 (2014), pp-1695-1699.

[12] Electronic Archive: New Semiconductor Materials, Characteristics and properties. [Online]

[13] D. L. Scharfetter and H. K. Gummel, Large signal analysis of a Silicon Read diode oscillator, IEEE Trans on Electron Devices, Vol. 16 (1969), pp. 64-77.

[14] M. Gilden and M. E. Hines, Electronic tuning effects in the read microwave avalanche diodes, IEEE Trans. Electron Devices, Vol. 13 (1966),